I&EC research
Industrial & Engineering Chemistry Research

Article

Cite This: Ind. Eng. Chem. Res. 2019, 58, 3468−3477

pubs.acs.org/IECR

Investigation of Matrix Effects in Laboratory Studies of Catalytic Ozonation Processes

Wenwen Yang and Tingting Wu*

Department of Civil and Environmental Engineering, The University of Alabama in Huntsville, Huntsville, Alabama 35899, United States

Supporting Information

ABSTRACT: A systematic study investigating the effects of water matrices on heterogeneous catalytic ozonation processes was conducted in a semibatch reactor at initial pH 7.00 ± 0.20. Specifically, three matrices commonly used in laboratory studies were tested: deionized (DI) water, phosphate buffered solution, and *tetra*-borate buffered solution. Three metal oxide catalysts on SiO_2 support, CuO/SiO_2, Fe_2O_3/SiO_2, and MnO_2/SiO_2 (all ∼4.5% metal loading), were synthesized and used as representative solid catalysts. Oxalate was selected as the model compound as it is a common end product in aqueous ozonation processes and also a typical refractory compound to conventional chemical oxidation. Hydroxyl radical (•OH) is generally accepted as the main reactive species in catalytic ozonation processes and can react with oxalate by electron transfer. Catalytic ozonation of oxalate in different water matrices were carried out in a laboratory experimental setup where ozone concentrations in the feed gas and off gas line were continuously monitored. Decomposition tests with and without catalysts in different matrices were also conducted in batch homogeneous reactors to probe the matrix effects on ozone decomposition and interactions between ozone and the catalysts. Moreover, *t*-butanol (TBA) and methanol were added as the •OH probe compounds to investigate the oxalate degradation mechanisms in various matrices. It was found that the effects of water matrices on catalytic ozonation were multifaceted, including process performance, catalysts stability, and mechanism and reaction pathways. These matrix effects can be ascribed to the influence of inorganic anions such as phosphate and borate on ozone decomposition, competitive adsorption on the catalyst surface, and generation of reactive species during catalytic ozonation processes.

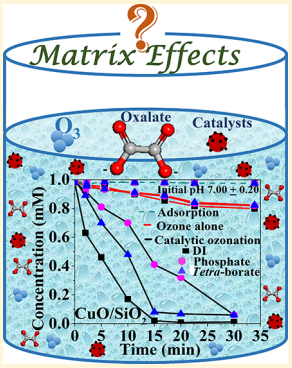

1. INTRODUCTION

Heterogeneous catalytic ozonation is one of the recommended advanced oxidation processes (AOPs) and has attracted much attention recently due to its capability of fast degradation and more efficient mineralization of many refractory organic compounds, shorter treatment time, and easy catalysts separation compared to homogeneous catalytic ozonation.[1−3] As some metal oxides (e.g., TiO_2, ZnO) have been frequently used in photocatalytic reduction of water pollutants,[4,5] metal oxides (e.g., MnO_2, CuO, Fe_3O_4) are also commonly used as the ozonation catalysts.[2,6,7] Moreover, Al_2O_3, Silica, ceramic honeycomb, and carbon nanotubes have been employed as the catalyst support owing to their large surface areas, chemical stability, and the ability to promote catalytic effects.[6−9]

In spite of the advantages and promising performance of heterogeneous catalytic ozonation, there are many contradictory results of research reported in the literature and the mechanism remains controversial.[10−12] These discrepancies and controversies may be resulted from the surface properties and/or stability of the catalyst, presence of natural organic matters, coexisting ions (e.g., carbonate and bicarbonate in natural water), and solution chemistries (e.g., pH).[12,13] The operating conditions particularly the nature of reactors can also influence the performance. In general, two types of reactors, batch and semibatch, are most commonly employed in laboratory catalytic ozonation studies. In batch reactor the working solution is presaturated with ozone or a stock ozone solution is diluted to the desired concentrations, whereas ozone is continuously dosed into the working solution in semibatch reactors.[9,14−18] In most studies, laboratory experiments were carried out in deionized (DI) water or well-controlled water matrices to facilitate mechanism investigations, where the pH was usually adjusted by acid/base[19,20] or buffered with phosphate[3,21]/*tetra*-borate.[22,23] While this seems to be a rational and valid research approach, the different solution chemical conditions of different controlled matrices may account for some of the reported controversies.

Heterogeneous catalytic ozonation can be a complex process which may involve mass transfer of gaseous ozone into the liquid phase as well as external and internal diffusion of ozone/solute into the solid catalysts. Enhanced generation of hydroxyl radicals (•OH), catalytic decomposition of O_3, and O_3 and organic compound interactions on the catalyst surface have been proposed as the possible catalytic mechanisms.[12,24] Also like many other AOPs, heterogeneous catalytic ozonation relies

Received: November 4, 2018
Revised: January 26, 2019
Accepted: February 4, 2019
Published: February 15, 2019

DOI: 10.1021/acs.iecr.8b05465
Ind. Eng. Chem. Res. 2019, 58, 3468−3477

on the generation of highly reactive radical species, typically •OH, which can oxidize organic pollutants quickly and nonselectively.[25] To enhance the efficiency of heterogeneous catalytic ozonation, many research efforts have been taken to develop various catalysts utilizing different surface modification processes, such as the impregnation of metal or metal oxides onto catalytic supports.[26,27] While most of these studies focused on evaluating the catalytic performance for the removal of selected refractory organic compounds under certain experimental conditions, much less attention has been paid to the effect of different water matrices on heterogeneous catalytic ozonation processes.[28]

Herein, we've conducted a systematic study aiming to explore and understand the effect of commonly used matrices on organic degradation during heterogeneous catalytic ozonation. Oxalate (OA) was selected as the target compound which underwent electron transfer with •OH ($k_{•OH/OA} = 5 \times 10^6$ (M^{-1} S^{1-})).[29] OA has been frequently used as the model compound in catalytic ozonation studies because it is a common end product in ozonation processes ($k_{O3} < 0.04$ M^{-1} S^{1-})[30] for water treatment and is also a typical refractory compound to conventional chemical oxidation. Three metal oxide based catalysts with silica support (CuO/SiO_2, Fe_2O_3/SiO_2, and MnO_2/SiO_2) were synthesized and used as the heterogeneous catalysts. Comparative experiments were conducted in three water matrices commonly used in laboratory ozonation studies, that is, DI water, phosphate buffered solution, and *tetra*-borate buffered solution, to investigate theirs effects on oxalate degradation during catalytic ozonation in a semibatch laboratory reactor. The stability of solid catalysts during ozonation in different matrices was also examined. The matrix effects on ozone/catalysts interactions and reaction mechanisms of oxalate degradation were explored.

2. EXPERIMENTAL SECTION

2.1. Materials and Reagents. Copper(II) nitrate trihydrate ($Cu(NO_3)_2 \cdot 3H_2O$, Acros Organics), Iron(III) nitrate nonahydrate ($Fe(NO_3)_3$ $9H_2O$, Acros Organic), and manganese nitrate ($Mn(NO_3)_2$, Acros Organic) were the sources of Cu, Fe, and Mn, respectively. Oxalic acid (Acros Organic) was used as the model compound. Potassium phosphate monobasic (KH_2PO_4, Fisher Scientific), potassium phosphate dibasic anhydrous (K_2HPO_4, Acros Organics), and sodium *tetra*-borate decahydrate ($Na_2B_4O_7$ $10H_2O$, Fisher Scientific) were used to prepare the two buffer solutions at a concentration of 5 mM for both phosphate and *tetra*-borate. *t*-Butanol (TBA) (Fisher Scientific) and methanol (Fisher Chemical) were employed as the radical scavengers. Hydrochloric acid (HCl, Acros Organics) and sodium hydroxide (NaOH, Fisher Scientific) were used to adjust the pH of the solutions. Spherical silica gel (S10040M, 70−200 μm) with a surface area of ∼100 m^2/g was obtained from Silicycle Inc., Canada and used as the catalyst support. Deionized water (DI water, 18.2 $M\Omega$ cm) was used for all synthesis and treatment processes.

2.2. Catalyst Preparation and Characterization. The solid catalysts used in this study were prepared using the incipient wetness impregnation method (IWI). Briefly, certain amount of spherical silica gel was added into a glass beaker, then the precursor solution ($Cu(NO_3)_2$, $Fe(NO_3)_3$, or $Mn(NO_3)_2$) was added with a volume equal to the total pore volume of the silica gel (0.9 mL/g). The mixture was mixed very well with a glass rod followed by sitting for 1 h and then dried in the oven at 120 °C for 10 h in air. Lastly, the mixture was moved to the furnace and calcined at 300 °C for 4 h in air with a heating rate of 5 °C/min. The products obtained were naturally cooled down to room temperature, then washed with DI water several times to remove any superficial or loosely bounded metal oxides, and finally dried in the oven at 80 °C. The metal loading was 45.6 ± 0.50 mg/g, 46.4 ± 0.50 mg/g, and 43.8 ± 0.50 mg/g for CuO/SiO_2, Fe_2O_3/SiO_2, and MnO_2/SiO_2, respectively (Supporting Information (SI) Text S1). X-ray diffraction (XRD) patterns of the catalysts were measured by a Rigaku MiniFlex 600 powder diffractometer with Cu Kα radiation, using a radiation at 40 kV and 15 mA. Two theta from 2° to 90° were obtained at a scanning rate of 0.5°/min. The surface composition of the catalysts and oxidation states of the elements were determined by X-ray photoelectron spectroscopy (XPS, Kratos analytical AXIS 165). The point of zero charge (pH_{pzc}) was determined using the pH drift method and the batch equilibrium technique, where 0.20 g of solids was added into 20 mL of 0.01 M NaCl solution and the initial pH was adjusted from 2 to 12 by adding NaOH or HCl (0.1N).[31]

2.3. Ozone Decomposition Experiments. Ozone decomposition experiments were performed in five 100 mL Erlenmeyer flasks, each containing 50 mL ozone saturated solution (4.0 ± 0.2 mg/L) in one of the matrices tested (e.g., phosphate buffer, *tetra*-borate buffer, and DI). The initial pH was adjusted to pH 7.00 ± 0.20. Detailed experimental procedure was described in the SI (Text S2). The dissolved ozone concentration (DO_3) in each flask was measured using the indigo method after 5, 10, 15, 20, and 30 min, respectively.

Ozone decomposition experiments in the presence of catalysts were performed similarly (SI Text S2), but with addition of 125 mg of catalysts into each flask. After a specific time interval (5, 10, 15, 20, and 30 min), one flask was opened and the solution was quickly split into two 25 mL suspensions consisting of reaction solution and catalyst particles. One suspension was quickly filtered through a Millipore filter (0.45 μm, PVDF), then the ozone concentrations of the filtrate and the other suspension were measured using the indigo method, where the difference was determined as the ozone that adsorbed onto the catalyst surface. To minimize the influence of filtration on aqueous ozone, the filter was rinsed with ozone saturated solution before sample filtration. Preliminary tests confirmed the negligible effects of filtration on aqueous ozone concentrations (SI Figure S2).

2.4. Catalytic Ozonation Experiments. The experimental setup of catalytic ozonation tests is illustrated in Figure 1. The heterogeneous catalytic ozonation was carried out in a 250

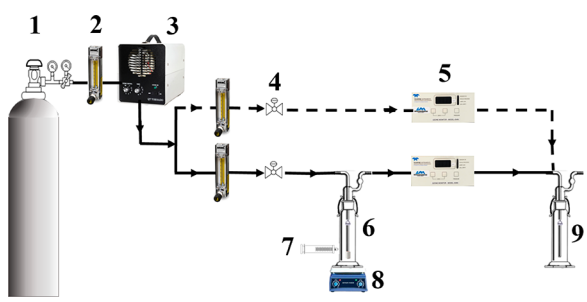

Figure 1. Experimental setup (1) O_2 gas cylinder, (2) flowmeter, (3) ozone generator, (4) valve, (5) gas ozone analyzer, (6) quartz reactor, (7) sampling port, (8) stirring plate, (9) 2% KI trap.

DOI: 10.1021/acs.iecr.8b05465
Ind. Eng. Chem. Res. 2019, 58, 3468−3477

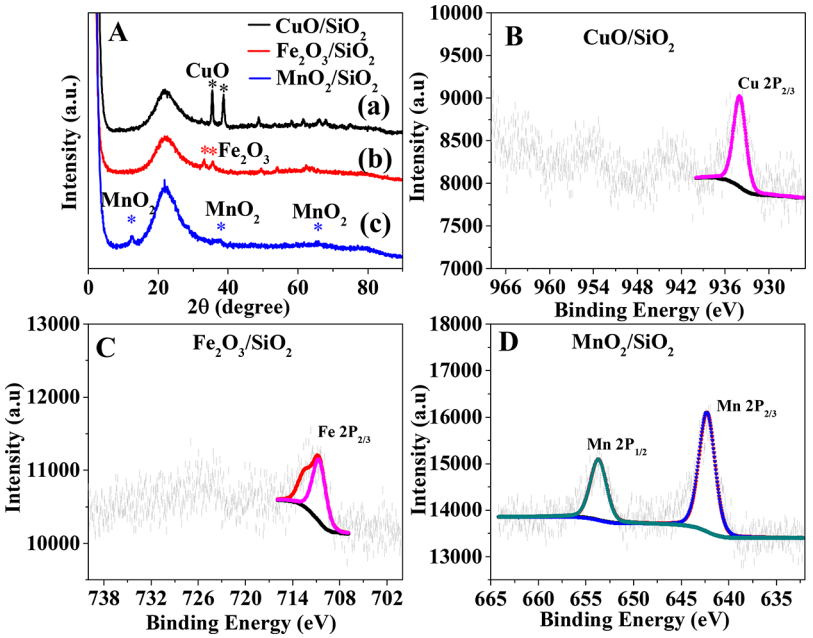

Figure 2. XRD patterns of CuO/SiO_2, Fe_2O_3/SiO_2, and MnO_2/SiO_2 (A); XPS spectra of CuO/SiO_2 (B), Fe_2O_3 (C), and MnO_2/SiO_2 (D) in Cu 2p, Fe 2p, and Mn 2p regions, respectively.

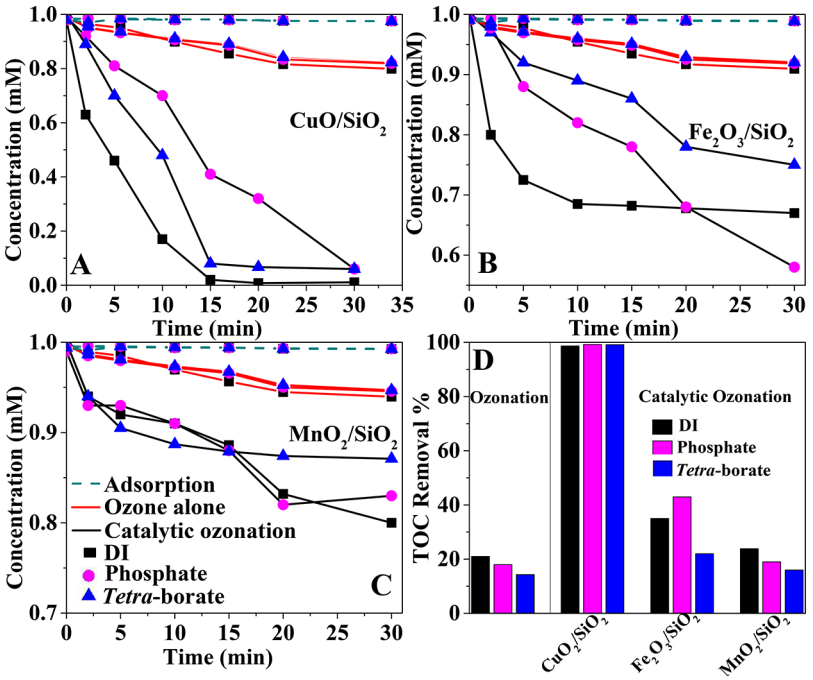

Figure 3. Oxalate degradation (A, B, C) and mineralization (D) in different water matrices. (Initial concentration: Oxalate, 1 mM, working solution: 200 mL, heterogeneous catalyst dose: 0.50 g, initial pH 7.00 ± 0.20, reaction time: 30 min.)

mL cylindrical quartz reactor. Pure oxygen (O_2) was used as the feeding gas and ozone (O_3) gas was generated by an ozone generator (MP5000, A2Z Ozone Inc., Louisville, KY). Typically, 0.50 g solid catalysts were added into 200 mL model compounds (1 mM oxalate) buffered solution (5 mM phosphate buffer or 5 mM *tetra*-borate buffer) or DI water at initial pH of 7.00 ± 0.20. The concentration of feeding O_3 (17.80 mg/L ± 0.05) was continuously monitored by passing a side stream ozone through an ozone analyzer (API-454). Ozone was injected into the working solution through a diffuser stone at a flow rate of 0.4 L/min (at working temperature and pressure). Samples were taken at predetermined time intervals for further analysis. At the end of each run, ozone supply was turned off and the working solution was purged with oxygen for another 5 min to remove any residual ozone in the system. Control experiments of ozonation were conducted under the same conditions without any catalysts. The transferred ozone was calculated from eq 1:

$$O_3\text{dosage[mg]} = \int_0^t (C_{\text{inlet}} - C_{\text{outlet}}) \times Q\,dt \quad (1)$$

DOI: 10.1021/acs.iecr.8b05465
Ind. Eng. Chem. Res. 2019, 58, 3468−3477

where C_{inlet} and C_{outlet} are ozone concentrations in the feeding line and off gas line respectively, mg/L; Q is gas flow into gas ozone analyzer, set at 0.4 L/min for all runs; t is the treatment time, min. The transferred ozone was calculated to be 10.20 ± 0.40 mg during the heterogeneous catalytic ozonation runs.

2.5. Analytic Methods. Oxalate were measured by HPLC (Agilent 1100 series) with a Hypersil Gold 100 × 2.1 mm C18 column and a diode array detector (DAD) at 210 nm. The mobile phase was 20 mM KH_2PO_4 and CH_3OH (97/3 v/v, pH was adjusted to 2.29 by phosphoric acid). Total organic carbon (TOC) was measured using Shimadzu TOC-LCPH. The concentrations of copper ions, total iron ions, and manganese ions were measured using Hach method 8506 (0.04−5.00 mg/L), 8008 (0.02−3.00 mg/L), 8034 (0.1−20 mg/L), respectively. The gaseous ozone concentration was measured by an API-454 ozone analyzer. The concentration of dissolved ozone was determined with the indigo method (Hach method 8311, 0.01−1.50 mg/L O_3 HR). All the experiments were performed at room temperature 22 ± 2 °C.

3. RESULTS AND DISCUSSION

3.1. Characteristics of the Catalysts. The XRD patterns of CuO/SiO_2, Fe_2O_3/SiO_2, and MnO_2/SiO_2 are shown in Figure 2. The peaks of 2θ at 35.42° and 38.65° are the characteristics of CuO (Figure 2A-a).[32] The peaks of 2θ at 33.2° and 35.6° are the characteristics of Fe_2O_3 (Figure 2A-b).[33] The weak peaks of MnO_2 at 13.2°, 37.45°, and 66° are ascribed to poor crystallized birnessite-type MnO_2 (Figure 2A-c).[34] The XRD of the silica sphere with a broad scattering maximum centered at 22.5° was also observed, which belongs to amorphous SiO_2.[35] The XPS analysis was further employed to obtain the chemical state information on CuO/SiO_2, Fe_2O_3/SiO_2, and MnO_2/SiO_2 catalysts. The XPS results are presented in Figure 2 (B, C, and D). For CuO/SiO_2 catalyst, the fitted peak at 933.6 eV is assigned to Cu $2p_{3/2}$ and the peak at 954.0 eV is assigned to Cu $2p_{1/2}$. The shakeup satellite peaks appeared at 942 and 944.0 eV, respectively (Figure 2B).[36] For Fe_2O_3/SiO_2 catalyst, the Fe $p_{3/2}$ and Fe $2p_{1/2}$ peaks were observed at 711.8 and 726.4 eV, respectively (Figure 2C).[37] For MnO_2/SiO_2 catalyst, two distinct peaks at banding energies of 644.5 and 656.4 eV were observed for Mn $2p_{3/2}$ and Mn $2p_{1/2}$, respectively (Figure 2D).[38] The pH_{pzc} of CuO/SiO_2, Fe_2O_3/SiO_2, and MnO_2/SiO_2 catalysts were found to be 5.70, 2.20, and 7.35, respectively.

3.2. Effects of Water Matrices on the Degradation of Oxalate (OA). Comparative catalytic ozonation experiments were conducted in different water matrices under otherwise identical conditions to examine the effects of water matrices on the degradation of oxalate. In addition, ozonation alone and adsorption tests were also carried out under the same conditions as control. As shown in Figure 3, less than 1∼2% of oxalate was adsorbed by the catalysts after 30 min, suggesting negligible contribution of adsorption to oxalate removal. More efficient removal of oxalate was achieved in the catalytic ozonation process with CuO/SiO_2 where >95% of oxalate was removed as compared to 20% by ozonation alone, while much less catalytic effects were observed for Fe_2O_3/SiO_2 and MnO_2/SiO_2 (Figures 3A, B, and C). The more effective oxalate removal using Cu-based catalysts was ascribed to the high complexation capacity of copper with oxalate. These copper-oxalate complexes may proceed oxidation and dissociation processes to form oxalate radical, which has a high reaction rate with molecular oxygen to form carbon dioxide and superoxide anion ($\bullet O_2$).[39,40] As for the effect of water matrices, the removal efficiency of oxalate with CuO/SiO_2 as the ozonation catalyst followed the order of DI > *tetra*-borate > phosphate. In contrast, the performance of Fe_2O_3/SiO_2 and MnO_2/SiO_2 in DI and phosphate buffered solution exceeded that of borate buffered one by 10∼20% within 30 min. In addition, longer experiments were conducted to better observe the asymptotic behavior during the runs of Fe_2O_3/SiO_2 in DI and MnO_2/SiO_2 in *tetra*-borate. As shown SI Figure S3, the OA degradation proceeded at a much slower rate after 10 ∼ 20 min, which means futile ozone decomposition (i.e., not resulting in OA degradation) became dominant in the system.

In addition to oxalate degradation, the degree of mineralization was also examined at the end of each run and the results are shown as TOC removal (Figure 3D). The measured TOC and calculated TOC based on OA concentrations were consistent within an allowable range of systematic error (SI Figure S4), indicating the intermediate products were either unstable (e.g., radicals) or indistinguishable from oxalate (e.g., Cu−oxalate complex) using the current analytical method (HPLC-DAD) or more likely a significant part of oxalate was mineralized in CO_2 and H_2O.[27,30,41,42]

3.3. Stability of Solid Catalysts. The stability of solid catalysts in aqueous solutions can sometimes be problematic in heterogeneous catalytic ozonation processes and need be carefully examined.[2,27] In this study, we monitored the metallic ion leaching as well as the pH evolution during the experiments (Figure 4). The leached Cu^{2+} concentration varied from 2.5 mg/L to 0.2 mg/L, Fe^{3+} from 0.34 mg/L to 0.02 mg/L, and Mn^{4+} from 1.0 mg/L to 0.6 mg/L. These results indicated that water matrices together with pH variation

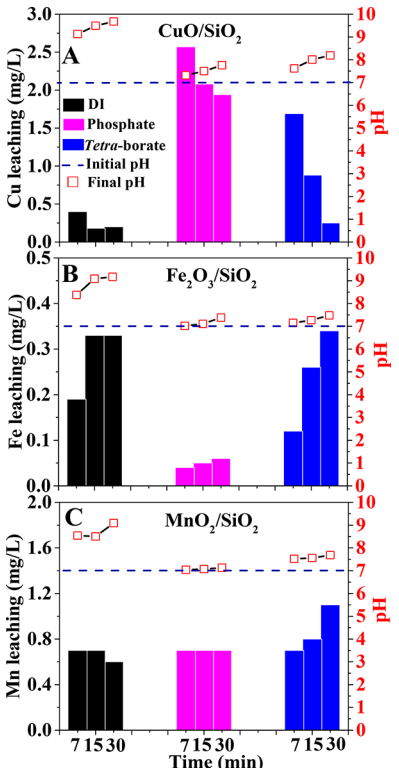

Figure 4. Metal leaching and pH evolution during catalytic ozonation of oxalate in different water matrices. (Initial concentration: oxalate, 1 mM; working solution: 200 mL, heterogeneous catalyst dose: 0.50 g, initial pH 7.00 ± 0.20.)

DOI: 10.1021/acs.iecr.8b05465
Ind. Eng. Chem. Res. 2019, 58, 3468−3477

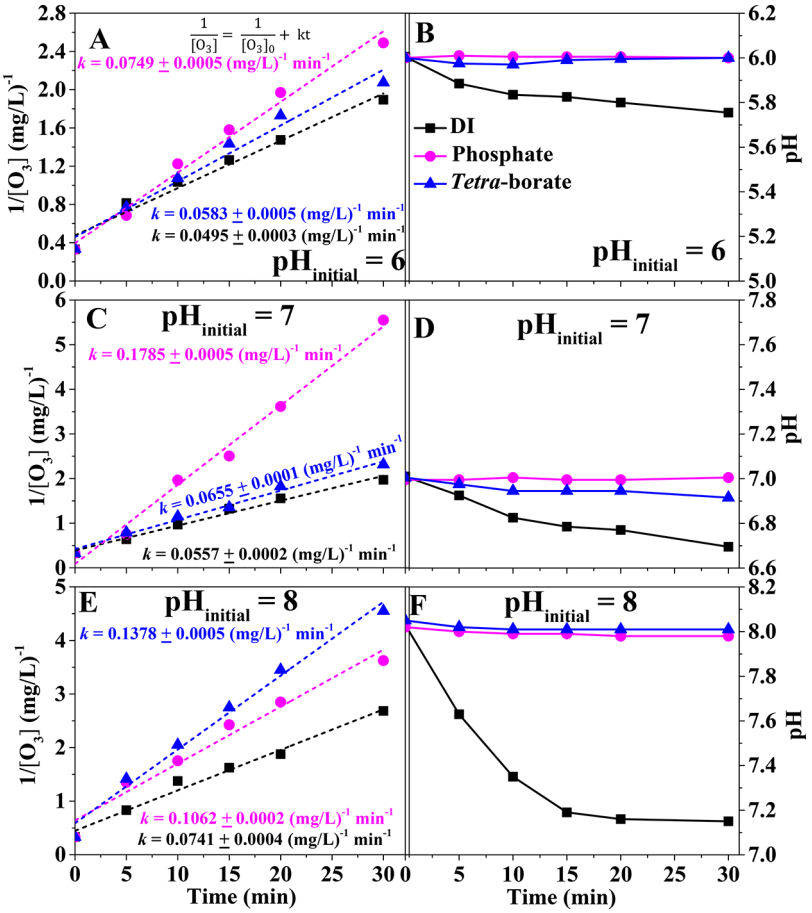

Figure 5. Kinetics of ozone decomposition (A, C, and E) and pH evolution (B, D, and F) in DI, phosphate buffered solution, and tetra-borate buffered solution. (Uncertainty represents one standard deviation derived from duplicate experiments.)

and interactions between oxalate and the catalysts (e.g., an unstable Cu (III)−oxalate complex formed through the reaction between •OH and Cu(II)−oxalate[41]) can affect the catalyst stability. On a closer look, the leached Cu^{2+} concentration decreased with time during catalytic ozonation of oxalate (Figure 4A), which may be because the pH increased during the test resulting in precipitation of some copper ions onto the solid catalysts. In contrast, Fe^{3+} and Mn^{4+} concentration generally increased with the reaction time. The low concentration of Fe^{3+} in phosphate buffered solution may be due to the low solubility of ferric phosphate. Moreover, small pH variation was observed in phosphate buffered solution due to its good buffering capacity in neutral pH range, whereas the pH increased more in DI and *tetra*-borate buffered matrices. This may partially explain the different stability of catalysts in different matrices. We further evaluated the possible contribution of homogeneous catalytic ozonation caused by the leached metal ions using the concentration of leached metal ions measured at 15 min (SI Figure S5). It turned out that the homogeneous catalytic effect caused by the metallic ions on the degradation of oxalate was insignificant except CuO/SiO_2 in phosphate buffered solution and Fe_2O_3/SiO_2 in tetra-borate buffered solution. These results indicated that the observed catalysis was mainly resulted from heterogeneous catalytic effects.

3.4. Effects of Water Matrices on Ozone Decomposition and Catalysts/Ozone Interactions. To understand the effect of water matrices on the interactions between catalysts and ozone, we first monitored ozone decomposition at initial pH of 6 ∼ 8 in different matrices without catalysts or the model compound as described in the Experimental section. As shown in Figure 5, the ozone decomposition generally followed a global second order kinetics. Faster ozone decomposition was achieved in the presence of phosphate/borate at all initial pH. The main reason is that the buffering capacity of these solutions can maintain a relatively constant pH during the run, whereas pH always dropped in DI due to consumption of OH^- by ozone decomposition. Moreover, ozone decomposition generally increased with increasing pH as it is well known that higher pH favors ozone decomposition. However, it is interesting to note one exception where the decomposition rate in phosphate at pH 7 ($k = 0.1785 \pm 0.0005$ $(mg/L)^{-1}$ min^{-1}) was higher than that at pH 8 ($k = 0.1062 \pm 0.0002$ $(mg/L)^{-1}$ min^{-1}). This implies that in addition to pH regulation, these inorganic ions may also interact with the radical chain reactions that lead to the decomposition of ozone. For phosphate ions (i.e., $H_2PO_4^-$ and HPO_4^{2-} at pH 6∼8), both promotion and inhibition of these chain reactions have been proposed in the literature. It was suggested that $H_2PO_4^-$ might participate as a proton source for the formation of ozonide radical HO_3•,[43,44] which is then converted to •OH and reacts with O_3.[45] On the other hand, phosphates are also considered as •OH scavengers and thus may inhibit ozone decomposition.[45−47] According to the results obtained here, it seems the relative importance of promotion and inhibition effects may be pH dependent. At pH ∼ 7, which is close to

DOI: 10.1021/acs.iecr.8b05465
Ind. Eng. Chem. Res. 2019, 58, 3468−3477

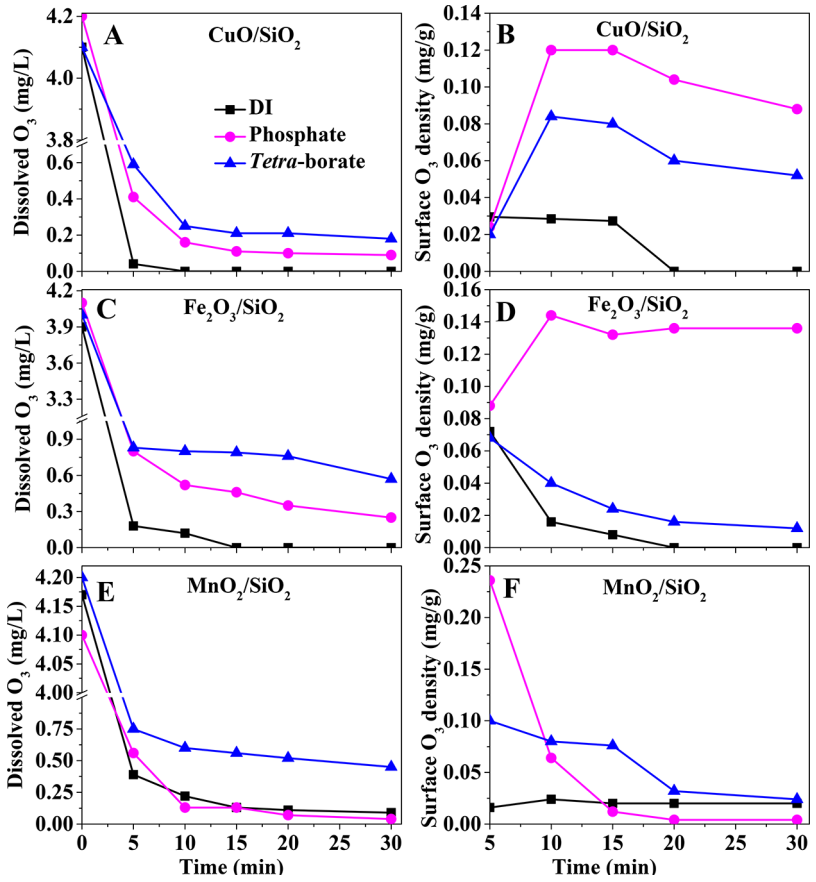

Figure 6. Changes of ozone concentration in aqueous solutions (A, C, and E) and the adsorbed ozone onto catalysts (B, D, and F) during the decomposition of ozone in different water matrices. (Working solution: 50 mL, heterogeneous catalyst dose: 0.125 g, initial pH 7.00 ± 0.20.)

pK_{a2} (7.21) of phosphoric acid, phosphate acts best as a buffer and may also serve as a very efficient proton source for the chain reactions, resulting in a high ozone decomposition rate; while at pH 8, •OH scavenging may overshadow such effect and slower the decomposition of ozone. The much enhanced decomposition rate in borate solution at pH ∼8 (doubles that at pH 7) could also be explained in a similar way, that is, pH ∼8 is closer to the pK_a (9) of $HB_4O_7^-$.

Next, the O_3 concentration in the aqueous phase (DO_3) as well as that adsorbed on the catalyst surface (surface O_3 density) during ozone decomposition in different water matrices were also measured in the presence of different catalysts. As can be seen in Figures 6(A, C, and E), DO_3 decreased by more than 80% in 5 min in all water matrices, which means ozone was either decomposed in the aqueous solution and/or adsorbed onto the catalysts (and subsequently decomposed). Furthermore, in contrast to ozone decomposition in the absence of catalysts (Figure 5), the highest DO_3 decay rate was observed in DI matrix especially for CuO/SiO_2 and Fe_2O_3/SiO_2 suspensions. This may be because the multivalent phosphate and tetra-borate ions may compete with O_3 for surface − OH sites on the metal oxides.[12,48,49] The surface O_3 density on CuO/SiO_2 and Fe_2O_3/SiO_2 generally corresponded with the changes of aqueous DO_3 concentrations during the first 10 min, i.e., as DO_3 decreased, the surface O_3 density increased. Moreover, the surface O_3 density was higher in the matrix of phosphate buffer than those in tetra-borate and DI matrices. At neutral pH, the surface of CuO_2/SiO_2 (pH_{pzc} 5.70) and Fe_2O_3/SiO_2 (pH_{pzc} 2.20) was negatively charged. Therefore, phosphate as a strong Lewis base was repelled from the catalyst surface due to electric repulsion, which may result in relatively less competition with O_3 for surface−OH sites and lead to faster DO_3 decrease and higher surface O_3 densities in phosphate matrices. The rapid decline of DO_3 and low surface O_3 densities in DI matrix might be ascribed to the abundant surface−OH sites available, where O_3 was adsorbed and decomposed quickly (less than 5 min). After it reached the maximum at ∼10 min, the surface O_3 density started to decrease as ozone decomposition exceeded adsorption. The relatively stable surface O_3 density on Fe_2O_3/SiO_2 in phosphate buffer might be because adsorption and desorption were in dynamic equilibrium.[3] The ozone adsorption and desorption behavior in the MnO_2/SiO_2 suspension was different than those in CuO_2/SiO_2 and Fe_2O_3/SiO_2 suspensions. The pH_{pzc} of MnO_2/SiO_2 (7.35) was close to the solution pH (∼7). In this case, most of the surface hydroxyl groups were at neutral state and thus enhanced the adsorption of ozone on the surface of MnO_2/SiO_2. Therefore, the surface O_3 density maximized in less than 5 min. Furthermore, the decomposition of adsorbed ozone can be accelerated by the reactions between ·OH and phosphate ions and enhanced electrons transfer shuttled by Mn(III)/Mn(IV).[8,50]

3.5. Effects of Water Matrices on the Reaction Mechanisms. In general during heterogeneous catalytic ozonation processes, either ozone or organic compounds or both should first be chemisorbed on the catalyst surface. The sorbed ozone may decompose and generate reactive species

DOI: 10.1021/acs.iecr.8b05465
Ind. Eng. Chem. Res. 2019, 58, 3468−3477

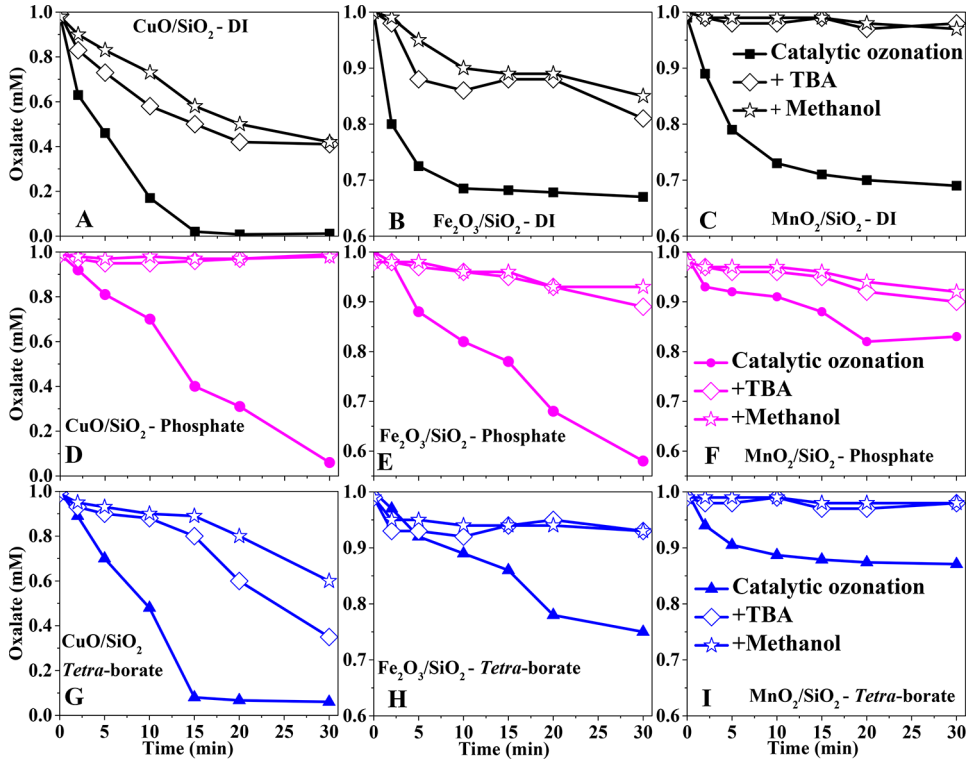

Figure 7. Oxalate degradation with and without *tert*-butanol (TBA) and methanol. (Initial oxalate: 1 mM; working solution: 200 mL, heterogeneous catalyst dose: 0.50 g, initial pH = 7.00 ± 0.20, *t*-butanol (TBA; when added): 0.325 mM, methanol (when added): 2 mM.)

(e.g., •OH) reacting with organic compounds that are also adsorbed on the catalysts or in the bulk solution, whereas chemisorption of the organic compounds may lower the energy barrier and enable reactions with molecular ozone.[12,11,28,51] Here, we used TBA and methanol as the probe compounds to investigate the generation of •OH during catalytic ozonation processes. TBA can quickly react with •OH (5×10^8 M^{-1} s^{-1})[15] in the bulk solution whereas methanol may react with both free and surface sorbed •OH (7×10^8 M^{-1} S^{1-}).[45] Therefore, the inhibition effects caused by the addition of TBA and methanol may help reveal the main reactive species responsible for oxalate degradation and further elucidate the role of free and bounded •OH. Moreover, it is worth mentioning that these probe compounds react much slower with ozone ($k_{O3/TBA} = 3 \times 10^{-3}$ M^{-1} s^{-1}; $k_{O3/CH3OH}$ = 0.024 M^{-1} s^{-1}).[15,52] The concentration profiles of gas ozone with and without scavengers were almost identical (SI Figure S6), which indicates the observed effects should be caused by scavenging of •OH rather than depletion of ozone by TBA/methanol. As shown in Figure 7A, D, and G, both TBA and methanol inhibited oxalate degradation in all matrices during catalytic ozonation with CuO/SiO_2 as the catalysts. However, in contrast to the almost complete inhibition in phosphate buffered solution (~5% removal with TBA/methanol vs 99% removal without TBA/methanol), ~55% oxalate was removed in the presence of TBA/methanol in DI matrix, and ~65% and ~40% was removed with the addition of TBA and methanol in tetra-borate buffered solution, respectively. These results indicate that in DI and borate matrices, both •OH and O_3 were the active species for oxalate degradation. The reaction with O_3 may occur through the formation of copper−oxalate complex on the catalyst surface. For the •OH pathway, it seems both surface sorbed and free •OH are involved as higher degree of inhibition was observed in the presence of methanol. Furthermore, the inhibition effect was more pronounced during the first ~15 min in borate solution which may be ascribed to the competition for surface sites between borate, ozone, and oxalate. In phosphate buffered solution (Figure 7D), free •OH appeared to be the dominant reactive species. On one hand, the formation of surface oxalate complex may be hindered due to the high affinity between phosphate and metal oxides, thus suppressing the O_3 reaction pathway; on the other hand, the leached copper ions (SI Figure S5D) can act as homogeneous catalysts which can propagate •OH generation in the bulk solution through O_3 decomposition in the bulk solution. The addition of probe compounds can scavenge •OH and terminate the reaction chain.[41]

For catalytic ozonation with Fe_2O_3/SiO_2 (Figure 7B, E, and H) and MnO_2/SiO_2 (Figure 7C, F, and I), similar inhibition effects were observed in all matrices with the addition of TBA and methanol, indicating free •OH might have played the dominant role in oxalate degradation. Moreover, unlike nearly complete inhibition of oxalate degradation in phosphate and borate buffered solutions (<10% removal), certain degree of removal was achieved in DI when Fe_2O_3/SiO_2 was used as the catalysts. This may be explained by the competitive adsorption of phosphate and borate on the catalyst surface which impeded the formation of surface complex and consequently the ozone reaction pathway as discussed above. In general, MnO_2/SiO_2 appeared to be much less efficient on catalytic ozonation of oxalate, which was somewhat further depressed in phosphate and borate matrices like when CuO/SiO_2 was the catalysts.

Reactions between oxalate and •OH typically occur through electron transfer,[29,53] which may be affected by the presence of other competitive species. For example, •OH can also react with inorganic ions via electron-transfer or hydrogen

DOI: 10.1021/acs.iecr.8b05465
Ind. Eng. Chem. Res. 2019, 58, 3468−3477

abstraction in aqueous solutions.[54] In phosphate or *tetra*-borate buffered matrices, the electron transfer reaction rate constants between •OH and the main inorganic ions are ~ 10^5 M^{-1} s^{-1} for $H_2PO_4^{1-}$/ HPO_4^{2-}, and 5.1 × 10^6 M^{-1} s^{-1} for *tetra*-borate.[55,56] Therefore, in addition to the competition between the multivalent ions (i.e., phosphate and borate) and ozone molecules for surface sites of the catalysts, these inorganic ions present in the matrices may also act like a •OH scavenger and inhibit oxalate degradation to certain degree. Furthermore, minimal catalytic effects were observed during oxalate ozonation with MnO_2/SiO_2 (Figure 3C), which may indicate that the decomposition of O_3 after the fast adsorption onto the catalyst surface was mostly futile decomposition which did not lead to efficient reactive species generation. Moreover, oxalate as an anionic species can be adsorbed on slightly positively charged MnO_2/SiO_2 via electrostatic interactions instead of surface complexation. Therefore, when MnO_2/SiO_2 was used as the catalysts, the limited free •OH responsible for oxalate degradation in different matrices (Figure 7C, F, and I) were mostly from the decomposition of DO_3 in the bulk water. This is also supported by the results that compared with ozonation alone, catalytic ozonation with MnO_2/SiO_2 only achieved 5 ~15% more removal (Figure 3C).

4. CONCLUSIONS

In this research effort, we conducted a systematic study to investigate the effects of commonly used laboratory matrices on the catalytic ozonation of a model compound, oxalate. CuO/SiO_2, Fe_2O_3/SiO_2, and MnO_2/SiO_2 were synthesized via incipient wetness impregnation methods and used as representative solid catalysts. In addition to oxalate degradation, the stability of solid catalysts, the interactions between catalysts and ozone, and the reaction mechanisms were also examined and explored. The catalysts showed different stability in different matrices and under certain circumstances (e.g., CuO/SiO_2 in phosphate buffered solution and Fe_2O_3/SiO_2 in tetra-borate buffered solution) the homogeneous catalytic effects caused by the leached metallic ions also contributed to the removal of oxalate. In the absence of catalysts or model compounds, the decomposition of ozone was generally accelerated in buffering solutions and such promotion effects may be maximized at pH close to the pK_a of the inorganic ions. While the presence of solid catalysts accelerated the depletion of dissolved ozone, the ozone decomposition rates as well as surface ozone density on the catalysts were affected by the matrices. In contrast to ozone decomposition in the absence of catalysts, higher DO_3 decay rate was observed in DI matrix because the inorganic ions may compete with O_3 for surface−OH sites on the metal oxides. TBA and methanol were used as the probe compounds to investigate the reactive species for oxalate removal. Hydroxyl radicals (free and/or surface sorbed) were found to play an important role in oxalate degradation in all solutions, whereas inorganic ions present in the matrices may act like a •OH scavenger and inhibit oxalate degradation to certain degree. Water matrices may also influence other reaction pathways of catalytic ozonation such as the formation of surface complex.

All these results indicate that the water matrices not only provide the buffering capacities, but also affect the catalytic ozonation process in various aspects, which may not be neglected in laboratory studies. While the selection of water matrices may essentially depend on the focus, requirements, and objectives of specific studies, we believe this study can provide new insights into the investigation of heterogeneous catalytic ozonation processes, facilitate experiment design for the development and evaluation of new catalysts, and further expedite the transition of heterogeneous catalytic ozonation processes from laboratory studies to practical applications in water and wastewater treatment.

■ ASSOCIATED CONTENT

Supporting Information

The Supporting Information is available free of charge on the ACS Publications website at DOI: 10.1021/acs.iecr.8b05465.

Metal loading test (Text S1), ozone decomposition experiments (Text S2); comparison of the dissolved ozone concentration in different flask (Figure S1); comparison of the dissolved ozone concentration before and after filtration (Figure S2); oxalate degradation during longer experiments runs of Fe_2O_3/SiO_2 in DI and MnO_2/SiO_2 in *tetra*-borate (Figure S3); measured TOC vs calculated TOC of OA after 30 min treatment (Figure S4); comparison of heterogeneous and homogeneous catalytic ozonation (Figure S5); comparison of the gas ozone in the feeding line and off gas line during the runs with and without TBA/CH_3OH (Figure S6) (PDF)

■ AUTHOR INFORMATION

Corresponding Author

*Phone: +1-256-824-6423; e-mail: Tingting.Wu@uah.edu.

ORCID

Tingting Wu: 0000-0002-4653-8493

Notes

The authors declare no competing financial interest.

■ ACKNOWLEDGMENTS

This study was supported by the U.S. National Science Foundation (CBET-1606117). We thank Clint Cook and Nathan Perinovic for their assistance in the lab. We also thank the anonymous reviewers for their valuable comments and suggestions that helped improve the quality of the paper.

■ REFERENCES

(1) Kasprzyk-Hordern, B.; Ziółek, M.; Nawrocki, J. Catalytic ozonation and methods of enhancing molecular ozone reactions in water treatment. *Appl. Catal., B* **2003**, *46* (4), 639−669.

(2) Nawaz, F.; Cao, H.; Xie, Y.; Xiao, J.; Chen, Y.; Ghazi, Z. A. Selection of active phase of MnO2for catalytic ozonation of 4-nitrophenol. *Chemosphere* **2017**, *168*, 1457−1466.

(3) Yuan, L.; Shen, J.; Yan, P.; Chen, Z. Interface Mechanisms of Catalytic Ozonation with Amorphous Iron Silicate for Removal of 4-Chloronitrobenzene in Aqueous Solution. *Environ. Sci. Technol.* **2018**, *52* (3), 1429−1434.

(4) Zhao, Zengying; An, He; Lin, Jing; Feng, Mingchao; Murugadoss, Vignesh; Ding, Tao; Liu, Hu; Shao, Qian; Mai, Xianmin; Wang, Ning; Gu, Hongbo; Angaiah, Subramania; ZG. Progress on the Photocatalytic Reduction Removal of Chromium Contamination. *Chem. Rev.* **2018**, *18*, 1−11.

(5) Chong, Mengnan; jin, Bo; Chow, Christopher W. K.; Saint, C. Recent developments in photocatalytic water treatment technology: A review. *Water Res.* **2010**, *44*, 2997−3027.

(6) Petre, A. L.; Carbajo, J. B.; Rosal, R.; Garcia-calvo, E.; Perdigón-melón, J. A. CuO/SBA-15 catalyst for the catalytic ozonation of mesoxalic and oxalic acids. Water matrix effects. *Chem. Eng. J.* **2013**, *225*, 164−173.

(7) He, H.; Liu, Y.; Wu, D.; Guan, X.; Zhang, Y. Ozonation of dimethyl phthalate catalyzed by highly active CuxO-Fe3O4nanopar-

DOI: 10.1021/acs.iecr.8b05465
Ind. Eng. Chem. Res. 2019, 58, 3468−3477

ticles prepared with zero-valent iron as the innovative precursor. *Environ. Pollut.* **2017**, *227*, 73−82.
(8) Zhao, L.; Ma, J.; Sun, Z. Z.; Zhai, X. D. Catalytic ozonation for the degradation of nitrobenzene in aqueous solution by ceramic honeycomb-supported manganese. *Appl. Catal., B* **2008**, *83* (3−4), 256−264.
(9) Sui, M.; Xing, S.; Sheng, L.; Huang, S.; Guo, H. Heterogeneous catalytic ozonation of ciprofloxacin in water with carbon nanotube supported manganese oxides as catalyst. *J. Hazard. Mater.* **2012**, *227−228*, 227−236.
(10) Nawrocki, J.; Kasprzyk-Hordern, B. The efficiency and mechanisms of catalytic ozonation. *Appl. Catal., B* **2010**, *99* (1−2), 27−42.
(11) Nawrocki, J. Catalytic ozonation in water: Controversies and questions. Discussion paper. *Appl. Catal., B* **2013**, *142−143*, 465−471.
(12) Kasprzyk-hordern, B.; Ziółek, M.; Nawrocki, J. Catalytic ozonation and methods of enhancing molecular ozone reactions in water treatment. *Appl. Catal., B* **2003**, *46*, 639−669.
(13) Zhao, L.; Ma, W.; Lu, S.; Ma, J. Influencing investigation of metal ions on heterogeneous catalytic ozonation by ceramic honeycomb for the degradation of nitrobenzene in aqueous solution with neutral pH. *Sep. Purif. Technol.* **2019**, *210*, 167−174.
(14) Legube, B.; Leitner, N. K. V. Catalytic ozonation: a promising advanced oxidation technology for water treatment. *Catal. Today* **1999**, *53* (1), 61−72.
(15) Gunten, U. Ozonation of Drinking Water Part I Oxidation Kinetics and Product Formation. *Water Res.* **2003**, *37*, 1443−1467.
(16) Mcdowell, D. C.; Huber, M. M.; Wagner, M. Ozonation of Carbamazepine in Drinking Water: Identification and Kinetic Study of Major Oxidation Products. *Environ. Sci. Technol.* **2005**, *39* (20), 8014−8022.
(17) Shiraga, M.; Kawabata, T.; Li, D.; Shishido, T. Memory effect-enhanced catalytic ozonation of aqueous phenol and oxalic acid over supported Cu catalysts derived from hydrotalcite. *Appl. Clay Sci.* **2006**, *33*, 247−259.
(18) Zhuang, H.; Han, H.; Hou, B.; Jia, S.; Zhao, Q. Heterogeneous catalytic ozonation of biologically pretreated Lurgi coal gasification wastewater using sewage sludge based activated carbon supported manganese and ferric oxides as catalysts. *Bioresour. Technol.* **2014**, *166*, 178−186.
(19) Abdedayem, A.; Guiza, M.; Ouederni, A. Comptes Rendus Chimie Copper supported on porous activated carbon obtained by wetness impregnation: Effect of preparation conditions on the ozonation catalyst ' s characteristics´ par un charbon actif obtenu Un catalyseur au cuivre supporte´ gnation pa. *C. R. Chim.* **2015**, *18* (1), 100−109.
(20) Nawaz, F.; Cao, H.; Xie, Y.; Xiao, J.; Chen, Y.; Ali, Z. Selection of active phase of MnO 2 for catalytic ozonation of 4-nitrophenol. *Chemosphere* **2017**, *168*, 1457−1466.
(21) Chen, K.; Wang, Y. The effects of Fe − Mn oxide and TiO 2/a -Al 2 O 3 on the formation of disinfection by-products in catalytic ozonation. *Chem. Eng. J.* **2014**, *253*, 84−92.
(22) Ã, Y. P.; Schumacher, J.; Jekel, M. Decomposition of aqueous ozone in the presence of aromatic organic solutes. *Water Res.* **2005**, *39*, 83−88.
(23) Thalmann, B.; Voegelin, A.; Von Gunten, U.; Behra, R.; Morgenroth, E.; Kaegi, R. Effect of Ozone Treatment on Nano-Sized Silver Sulfide in Wastewater Effluent. *Environ. Sci. Technol.* **2015**, *49* (18), 10911−10919.
(24) Comninellis, C.; Kapalka, A.; Malato, S.; Parsons, S. A.; Poulios, I.; Mantzavinos, D. Advanced oxidation processes for water treatment: advances and trends for R&D. *J. Chem. Technol. Biotechnol.* **2008**, *83* (6), 769−776.
(25) Gardoni, D.; Vailati, A.; Canziani, R. Decay of Ozone in Water: A Review. *Ozone: Sci. Eng.* **2012**, *34* (4), 233−242.
(26) Ghuge, S. P.; Saroha, A. K. Catalytic ozonation for the treatment of synthetic and industrial effluents - Application of mesoporous materials: A review. *J. Environ. Manage.* **2018**, *211*, 83−102.
(27) Huang, Y.; Sun, Y.; Xu, Z.; Luo, M.; Zhu, C.; Li, L. Removal of aqueous oxalic acid by heterogeneous catalytic ozonation with MnOx/sewage sludge-derived activated carbon as catalysts. *Sci. Total Environ.* **2017**, *575*, 50−57.
(28) Ernst, M.; Lurot, F.; Schrotter, J. C. Catalytic ozonation of refractory organic model compounds in aqueous solution by aluminum oxide. *Appl. Catal., B* **2004**, *47* (1), 15−25.
(29) Schworer, F.; Markovic, V. M.; Sehested, K. Pulse Radiolysis of Oxalic Acid and Oxalates. *J. Phys. Chem.* **1971**, *75* (6), 749−755.
(30) Sun, Q.; Li, L.; Yan, H.; Hong, X.; Hui, K. S.; Pan, Z. Influence of the surface hydroxyl groups of MnOx/SBA-15 on heterogeneous catalytic ozonation of oxalic acid. *Chem. Eng. J.* **2014**, *242*, 348−356.
(31) Órfão, J. J. M.; Silva, A. I. M.; Pereira, JC V; Barata, S. A.; Fonseca, I. M.; Faria, P. C. C. Adsorption of a reactive dye on chemically modified activated carbons — Influence of pH. *J. Colloid Interface Sci.* **2006**, *296*, 480−489.
(32) Ling, L. I. N.; Pengbin, P. A. N.; Zhangfeng, Z.; Zhaoji, L. I.; Jinxia, Y.; Minling, S. U. N.; Yuangen, Y. A. O. Cu/SiO 2 Catalysts Prepared by the Sol-Gel Method for Hydrogenation of Dimethyl Oxalate to Ethylene Glycol. *Chinese J. Catal.* **2011**, *32* (6), 957−969.
(33) He, Z.; Qian, Q.; Zhang, Z. Synthesis of higher alcohols from CO_2 hydrogenation over a $PtRu/Fe_2O_3$ catalyst under supercritical condition Subject Areas. *Phil Trans R Soc. A* **2015**, *373*, 1−10.
(34) Graphene, H. M. N.; Wu, Z.; Ren, W.; Wang, D.; Li, F.; Liu, B.; Cheng, H. High-Energy MnO 2 Nanowire/Graphene and Graphene Asymmetric Electrochemical Capacitors. *ACS Nano* **2010**, *4* (10), 5835−5842.
(35) Liou, T.; Chang, F.; Lo, J. Pyrolysis Kinetics of Acid-Leached Rice Husk. *Ind. Eng. Chem. Res.* **1997**, *36*, 568−573.
(36) Qi, F.; Chu, W.; Xu, B. Ozonation of phenacetin in associated with a magnetic catalyst CuFe 2 O 4: The reaction and transformation. *Chem. Eng. J.* **2015**, *262*, 552−562.
(37) Sun, B. Z.; Yuan, H.; Liu, Z.; Han, B.; Zhang, X. A highly Efficient Chemical sensor Material for H 2 S: a -Fe 2 O 3 Nanotubes Fabricated Using Carbon Nanotube Templates **. *Adv. Mater.* **2005**, *17*, 2993−2997.
(38) Manganese-tuned chemical etching of a platinumecopper nanocatalyst with platinum- rich surfaces. *J. Power Sources* **2016**;*304*:74−80. doi:.
(39) Zhang, T.; Li, W.; Croué, J. P. A non-acid-assisted and non-hydroxyl-radical-related catalytic ozonation with ceria supported copper oxide in efficient oxalate degradation in water. *Appl. Catal., B* **2012**, *121−122*, 88−94.
(40) Petre, A. L.; Carbajo, J. B.; Rosal, R.; García-calvo, E.; Letón, P.; Perdigón-melón, J. A. Applied Catalysis B: Environmental Influence of water matrix on copper-catalysed continuous ozonation and related ecotoxicity. *Appl. Catal., B* **2015**, *163*, 233−240.
(41) Yang, W.; Vogler, B.; Lei, Y.; Wu, T. Metallic ion leaching from heterogeneous catalysts: An overlooked effect in the study of catalytic ozonation processes. *Environ. Sci. Water Res. Technol.* **2017**, *3* (6), 1143−1151.
(42) Beltra, F. J.; Rivas, F. J. Ozone-Enhanced Oxidation of Oxalic Acid in Water with Cobalt Catalysts. 1. Homogeneous Catalytic Ozonation. *Ind. Eng. Chem. Res.* **2003**, *42*, 3210−3217.
(43) Ferre-Aracil, J.; Cardona, S. C.; Navarro-Laboulais, J. Kinetic study of ozone decay in homogeneous phosphate-buffered medium. *Ozone: Sci. Eng.* **2015**, *37* (4), 330−342.
(44) Buehler, R. E.; Staehelin, J.; Hoigne, J. Ozone decomposition in water studied by pulse radiolysis. 1. Perhydroxyl (HO2)/hyperoxide (O2-) and HO3/O3- as intermediates. *J. Phys. Chem.* **1984**, *88* (12), 2560−2564.
(45) Staehelin; Hoigné. Decomposition of Ozone in Water in the Presence of Organic Solutes Acting as Promoters and Inhibitors of Radical Chain Reactionst. *Environ. Sci. Technol.* **1985**, *19* (12), 1206−1213.

DOI: 10.1021/acs.iecr.8b05465
Ind. Eng. Chem. Res. 2019, 58, 3468−3477

(46) Morozov, P. A.; Ershov, B. G. The influence of phosphates on the decomposition of ozone in water: Chain process inhibition. *Russ J. Phys. Chem. A* **2010**, *84* (7), 1136−1140.
(47) Bińi, A. K.; Machniewski, P.; Wołyniec, J.; Pieńczakowska, A. Modeling of Ozone Reaction with Benzaldehyde Incorporating Ozone Decomposition in Aqueous Solutions. *Ozone: Sci. Eng.* **2013**, *35* (6), 489−500.
(48) Zhao, H.; Dong, Y.; Wang, G.; Jiang, P.; Zhang, J.; Wu, L.; Li, K. Novel magnetically separable nanomaterials for heterogeneous catalytic ozonation of phenol pollutant: NiFe 2 O 4 and their performances. *Chem. Eng. J.* **2013**, *219*, 295−302.
(49) Sun, Q.; Li, L.; Yan, H.; Hong, X.; Hui, K. S.; Pan, Z. Influence of the surface hydroxyl groups of MnO x/SBA-15 on heterogeneous catalytic ozonation of oxalic acid. *Chem. Eng. J.* **2014**, *242*, 348−356.
(50) Zhao, H.; Dong, Y.; Jiang, P.; Wang, G.; Zhang, J.; Li, K.; Feng, C. An α-MnO2nanotube used as a novel catalyst in ozonation: Performance and the mechanism. *New J. Chem.* **2014**, *38* (4), 1743−1750.
(51) Dai, Q.; Wang, J.; Yu, J.; Chen, J.; Chen, J. Applied Catalysis B: Environmental Catalytic ozonation for the degradation of acetylsalicylic acid in aqueous solution by magnetic CeO 2 nm catalyst particles. *Appl. Catal., B* **2014**, *144*, 686−693.
(52) Grima, N. M. M. Kinetic and mass transfer studies of ozone degradation of organics in liquid/gas- ozone and liquid/solid-ozone systems; Univ Bradford: UK, 2009.
(53) Li, K. E.; Crittenden, J. Computerized Pathway Elucidation for Hydroxyl Radical-Induced Chain Reaction Mechanisms in Aqueous Phase Advanced Oxidation Processes. *Environ. Sci. Technol.* **2009**, *43* (8), 2831−2837.
(54) Gligorovski, S.; Strekowski, R.; Barbati, S.; Vione, D.; Universite, A.; Umr, L. C. E. Environmental Implications of Hydroxyl Radicals (• OH). *Chem. Rev.* **2015**, *115*, 13051−13092.
(55) Dorfman, Leon M.; Aldamn, G. E. Reactivity of the Hydroxyl radical in Aqueous solution. *US Dep Commer Natl. Bur Standars.* **1974**, 1−59.
(56) Verberne, J. B. A Pluse Radiolysis Study of the Electron Reaction With DNA in Aqueous Solution and Ice. *Amsterasm.* **1981**, 1−209.

DOI: 10.1021/acs.iecr.8b05465
Ind. Eng. Chem. Res. 2019, 58, 3468−3477